16th ICAAR LISBOA 2020-2022

16th International Conference on
Alkali-Aggregate Reaction in Concrete
Lisboa | LNEC | Portugal | 31 May - 2 June 2022

http://icaar2020-2022.lnec.pt

Expansion prediction for alkali-silica reaction of concrete under real environmental and confinement conditions

Xi Ji [(1)], Yuya Takahashi [(2)]

(1) The University of Tokyo, Tokyo, Japan, ji@concrete.t.u-tokyo.ac.jp

(2) The University of Tokyo, Tokyo, Japan, takahashi@concrete.t.u-tokyo.ac.jp

Abstract

This research aims to improve existing prediction models for alkali–silica reaction (ASR) in concrete structures under real environmental and confinement conditions. Using a chemo-hygral multi-scale analytical system developed by the authors, ASR expansion progress of real-scale reinforced concrete (RC) bridge deck specimens under ambient conditions was simulated in a previous study. However, there were gaps between the simulation and measurement results in the quantitative expansion progress, due to insufficient consideration of parameters affecting the ASR. In this study, the performance of the existing model for simulating the dependencies of relative humidity (RH), temperature, and three-dimensional confinement was investigated by referring to previous experimental results. The RH and temperature dependencies on ASR can be simulated well with a slight modification to existing equations. The simulation results revealed that insufficient consideration of the relationship between the compressive stress and ASR gel absorption into pores might lead to gaps between the simulation and experimental results for the RC bridge deck specimens. Considering the different behavior of ASR gel absorption into pores, the experimental trends observed under realistic confinement conditions can be reproduced in the simulations. Clear ideas on how to modify the models in the future can be understood by visualizing the stress distribution in the simulation results for experiments under different confinement conditions.

Keywords: *alkali-silica reaction; prediction model; expansion; stress dependency; relative humidity dependency*

1. INTRODUCTION

Alkali–silica reactions (ASR) is a major cause of deterioration in concrete structures. ASR gel, which is formed through a reaction between alkaline pore solution and silica in aggregate, absorbs water and expands, gradually forming cracks in the concrete. The governing factors that affect ASR have been investigated by many researchers. For example, the temperature and moisture conditions of the surrounding environment affect the rate of ASR gel generation. The study conducted by Deschenes *et al.* [1] indicated that the threshold of relative humidity (RH) at which ASR occurs, varies with ambient temperature. A series of experiments was conducted by Gautam *et al.* [2] to investigate the relationship between multiaxial stress conditions and three-dimensional ASR expansion. The effect of these factors should be considered when assessing the service life of concrete structures damaged by ASR.

Numerical models, to predict ASR expansions based on the chemo-hygral computational system, were developed in the previous research conducted by Takahashi *et al.* [3]. However, the model still has difficulty in the quantitative prediction of the expansion of a real-scale reinforced concrete (RC) bridge deck on steel girders exposed to the outdoor environment [4]. Initially, this study examined the temperature, RH and confinement dependencies of ASR in the current model in comparison to the previous experimental results ([2], [5]). After slightly modifying the models, the prediction of the expansion of real-scale RC bridge deck was attempted again, and the performance of the prediction model was more comprehensively analyzed. This research attempts to provide ideas for further modification of the prediction model and aims to achieve accurate predictions of ASR in real environmental and confinement conditions.

2. PREVIOUS SIMULATION WITH ASR PREDICTION MODEL

2.1 Analytical model for ASR

This study used the multiscale analytical system for concrete structures, DuCOM-COM3, which was developed by Maekawa *et al.* [6] (Figure 2.1). This system is composed of a thermodynamic analytical system, DuCOM, and a nonlinear structural analytical system, COM3, to achieve the coupled calculation of both chemical and physical phenomena in concrete. The ASR model was developed by Takahashi *et al.* [3], and the global controlling parameters for both thermodynamic system and structural system were used in the calculation of ASR. For example, the water and alkali content in the thermodynamic system were used in the ASR kinetics model in the structural system and the consumption of these reactants was returned to the thermodynamic system. The models for ASR calculation related in this study are explained in the following sections. Other details of the models can be found in [3].

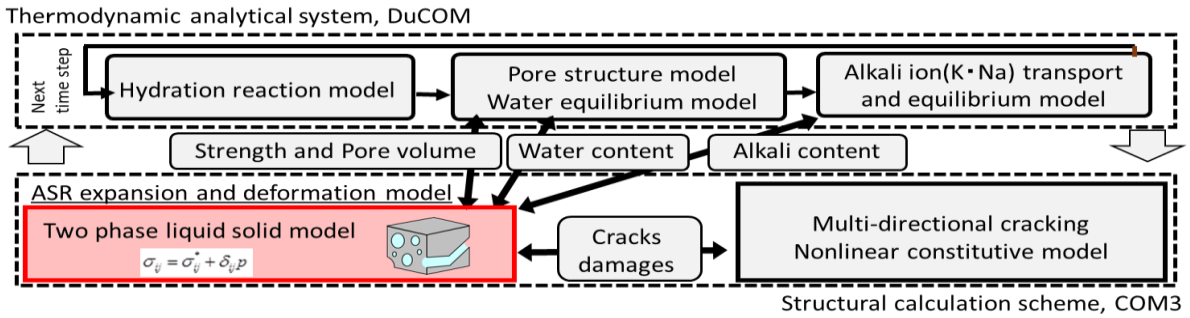

Figure 2.1: Overview of material-structural coupling system, DuCOM-COM3 [3,6]

2.1.1 ASR gel generation rate

The ASR gel generation rate ($\boldsymbol{R}_{X+}$ [mol/cm^3/s]) in each time step is formulated using Eqs. (1)–(4). The referential ASR gel generation rate $\boldsymbol{R}'_{X+}$ [mol/cm^3/s] in Eq. (1) is dominated by alkali concentration in the pore water ($\boldsymbol{C}_X$ [mol/l]), free water content ($\boldsymbol{F}_{water}$ [kg/m^3]), and reactive aggregate mass ($\boldsymbol{V}_{RG}$ [kg/m^3]). The ASR gel generation rate was calculated considering RH k_{RH} (Eq. (2)) and temperature dependencies k_T (Eq. (3)). The RH dependency equation represents the decrease of ASR in lower than humidity-saturated conditions, as illustrated in Figure 2.2. The temperature dependency equation is based on the Arrhenius equation, and the influence factor of different temperatures is considered [4] (Figure 2.3). These two equations are formulated to combine the influence of environmental conditions on the ASR gel generation rate.

$$R'_{X+} = k \cdot C_X \cdot F_{water} \cdot V_{RG} \cdot 1.0E-9 \quad (1)$$

$$k_{RH} = \exp(-1500.0 \cdot (1.0 - RH)^{5.0}) \quad (2)$$

$$k_T = \begin{cases} \mathrm{f(T)}(T \geq T_{th}) \\ \max(f'(T_{th})(T - T_{th}) - f(T_{th}), 0.0)(T < T_{th}) \end{cases}, \mathrm{f}(x) = \exp\left\{6000\left(\frac{1}{x} - \frac{1}{313}\right)\right\} \quad (3)$$

$$R_{X+} = k_{RH} \cdot k_T \cdot R'_{X+} \quad (4)$$

where k is the ASR coefficient, RH is the relative humidity, T is the temperature [K], T_{th} is the threshold temperature that results in ASR rate reduction.

After getting ASR gel generation rate, the generated ASR gel volume at each step could be calculated by Eq. (5).

$$\Delta Gel_{X+} = \frac{R_{ASR\_X+} \cdot \Delta t \cdot M_{gel}}{\rho_{gel}} \quad (5)$$

where ΔGel_{X+} is the generated ASR gel volume at the time step, Δt is time interval between steps, M_{gel} is the molecular mass of ASR gel, ρ_{gel} is the density of ASR gel.

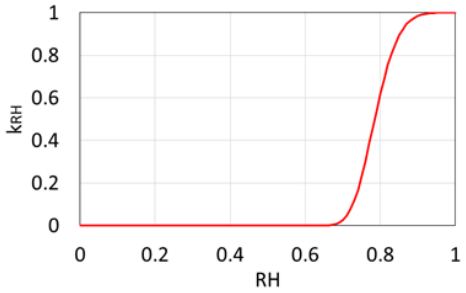

Figure 2.2: Relationship between k_{RH} and RH

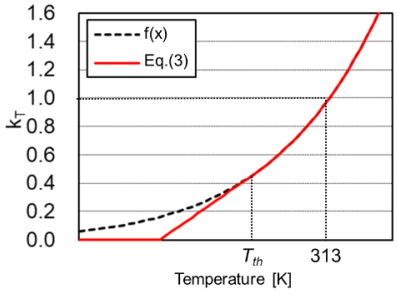

Figure 2.3: Temperature dependency model

2.1.2 ASR gel pressure calculations

In the ASR gel pressure calculations, models were formulated to consider the ASR gel absorption to capillary pores, and the coexistence of ASR gel in both solid and liquid phases [3].

To take into account the expansion under higher confinement conditions, ASR gel absorption into capillary pore was considered using Kelvin's equation (Eq. (6)). Additionally, the ASR gel volume that contributes to stress formation (V_{ASR}) was calculated by extracting absorbed gel (V_{pore}) from the total ASR gel volume. V_{pore} is expressed by Eq. (7) and illustrated in Figure 2.4. In a previous study, coefficient Z in Eq. (6) was considered constant, while it was found in the following section that Z is variable when the confinement state of the concrete structure changes. This is explained along with the trial simulation results in the next section.

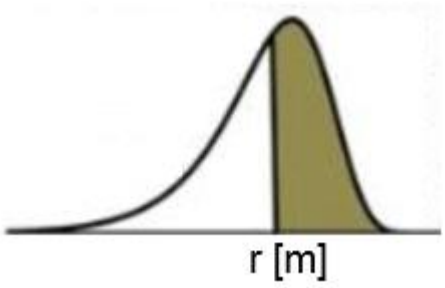

Figure 2.4: ASR gel absorption to pores [3]

$$\mathbf{r} = \frac{\mathbf{2Z}}{\mathbf{p}} \tag{6}$$

$$V_{pore} = \phi \exp\left(-\frac{r}{r_{peak}}\right) \tag{7}$$

where r is the minimum pore radius for ASR gel absorption [m], Z is the coefficient [m/Pa], p is the ASR gel pressure [Pa], ϕ is the porosity, r_{peak} is the peak radius of pore size distribution [m].

The ASR gel pressure (p [Pa], Eq. (8)) is calculated by combining the anisotropic pressure with the solid part of ASR gel (p_{ai} [Pa], Eq. (9)) and the isotropic pressure with the liquid part (p_i [Pa], Eq. (10)). The anisotropic and isotropic pressures are formulated based on the solid ratio in the ASR gel (β), existing ASR gel volume ($\boldsymbol{V_{asr}}$), and crack width in $\boldsymbol{i}$ direction ($\boldsymbol{V_{crack\_i}}$).

$$p = \frac{1}{3}\sum_i^{x,y,z} p_{ai} + p_i \tag{8}$$

$$p_{ai} = \mathrm{E} \cdot \beta \cdot \left(\frac{V_{asr}}{3} - V_{crack\_i}\right) \tag{9}$$

$$p_i = \mathrm{E} \cdot (1-\beta) \cdot \left(V_{asr} - \sum_{x,y,z} V_{crack\_i}\right) \tag{10}$$

where E is the stiffness of matrix and V_{crack_i} is the crack width in i direction.

2.2 Simulation of RC bridge deck

As a part of the author's previous research, expansion prediction simulations were attempted on a real-scale RC bridge deck specimen on steel girders exposed to outdoor environment [4]. This experiment was conducted to investigate the expansion behavior of concrete structures under ASR exposed to real environmental and confinement conditions. In the experiment, reactive coarse aggregate was used, and the mix proportion is shown in Table 2.1. Triaxial deformation of this bridge deck was measured with strain gauges embedded in certain positions, as shown in Figure 2.5. This bridge deck was exposed to real environmental conditions, and its temperature and RH were recorded daily.

Table 2.1: Mix proportion for the RC bridge deck [4]

W/C (%)	Air (%)	s/a (%)	Unit weight (kg/m^3)				Admixture (C ×%)		NaCl (kg/m^3)
			W	C	S	G	Water reducing agent	AE agent	
55.0	5.7	45.0	168	350	847	1977	1.0	0.001	18.9

The simulation of this bridge deck was conducted using the analytical models introduced in the previous section, using the recorded ambient temperature and RH as boundary conditions. The reactivity of the aggregate was derived from the sensitivity analyses using small prism specimens under free expansion. Considering the symmetry of the structure, one quarter of the structure was simulated. Figure 2.6 shows the comparison between the simulated and measured experimental results. There were gaps between the simulated and experimental expansion of the RC bridge; the simulated expansion in vertical direction is quite larger than experimental expansion, while the simulation could reproduce the deformation and crack directions of the specimen [4]. It was assumed that the problem was caused by the lack of proper equations describing the effect of RH, temperature, and multiaxial confinement.

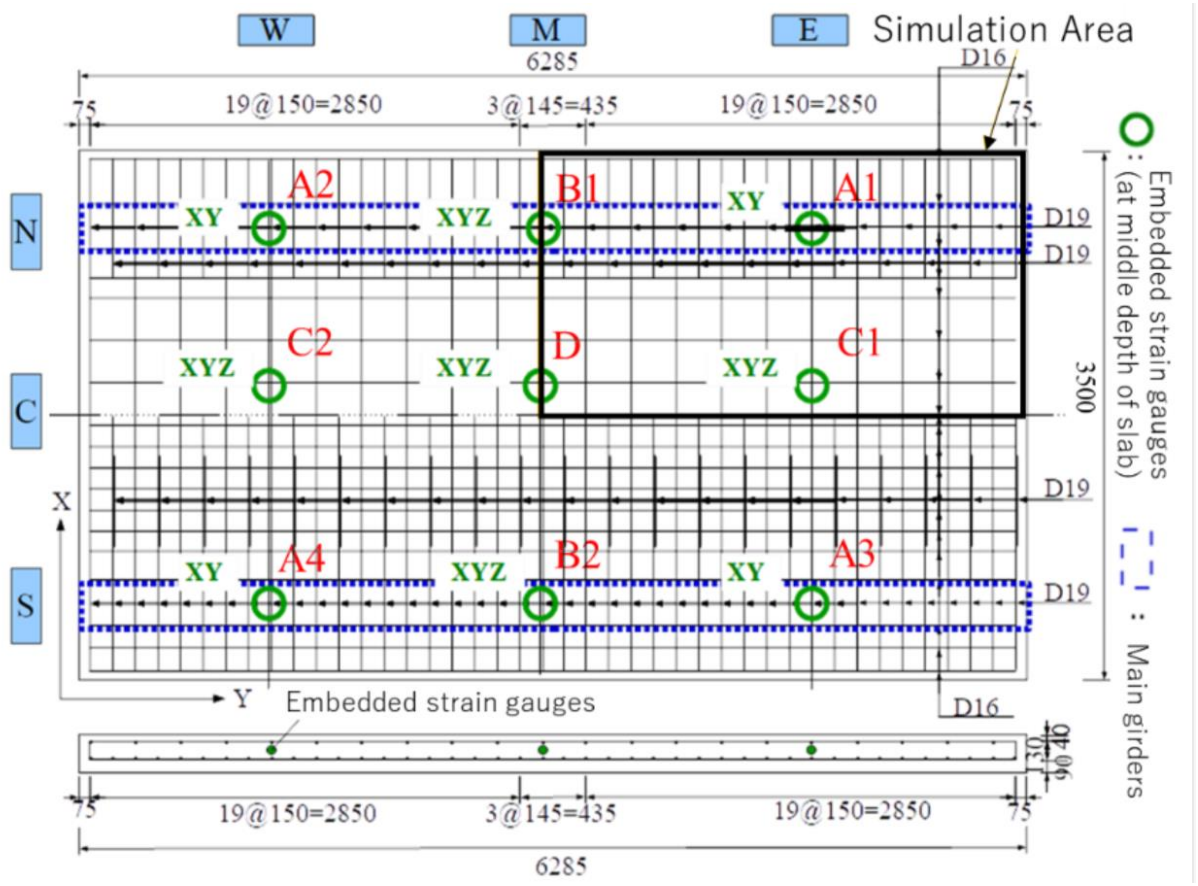

Figure 2.5: Reinforced steel arrangement, strain measurement, and simulation area [4]

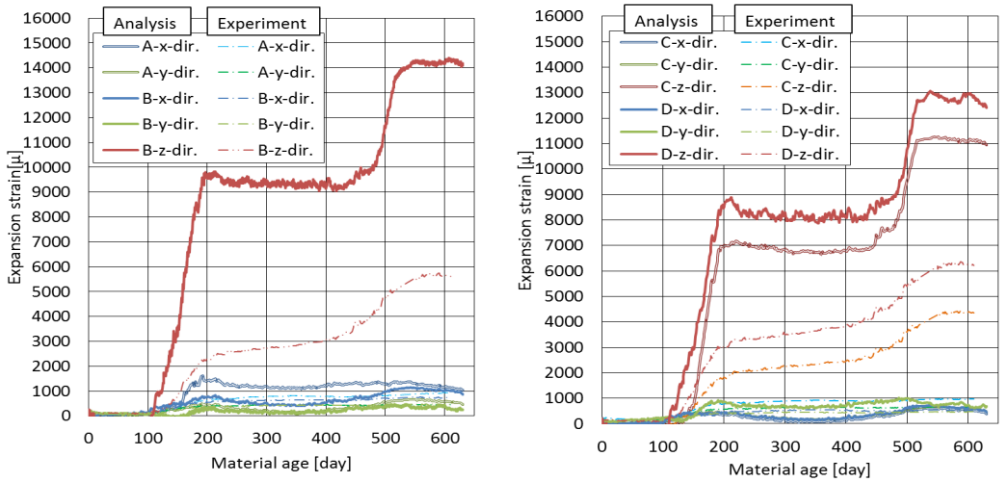

Figure 2.6: Simulated expansion of RC bridge deck [4]

3. SIMULATION OF DIFFERENT RELATIVE HUMIDITY AND TEMPERATURE CASES

3.1 Simulation of ASR experiment on relative humidity dependency

To investigate the performance of the current model on temperature and RH dependencies in ASR, the experiments conducted by Olaffson [5] were selected and simulated.

In the experiment by Olaffson [5], two groups of mortar specimens were stored in environmental conditions with temperatures of 23 ℃ and 38 ℃. In each group, the specimens were divided and set at different RHs, ranging from 73% to 100%. The test was performed according to ASTM C227. However, there is little information about mix proportion and curing conditions in this study. Thus, a mortar mix proportion shown in Table 3.1 was assumed as input for the simulated model. According to ASTM 227, the specimens were cured for 24 h at 23℃ . The analytical mesh used for simulation is shown in Figure 3.1. It has the same dimensions as the specimens.

The reactivity characteristics of the aggregate used in the experiment are not known. Using the expansion progress result for specimen at 38 ℃, RH 100%, sensitivity analyses was conducted to determine the characteristics of aggregate used in the experiment; parameter k in Eq. (1), average density of ASR gel, ρ_{gel} [g/cm^3] in Eq. (5), and the coefficient Z in Eq. (6) are the governing parameters for ASR kinetics and ASR gel characteristics and they were determined to be 0.0003, 3.0 and 3.0, respectively.

Table 3.1: Mix proportion used to simulate Olaffson's experiment [5]

W/C (%)	Unit weight (kg/m^3)			
50	W	C	S	Na_2O_{eq}
	295.5	591	1331	8.9

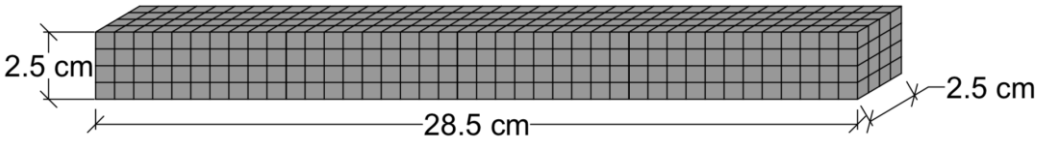

Figure 3.1: Mesh for mortar specimens

3.1.1 Results and discussion

Figure 3.2 shows the comparison between simulated and measured results for Olaffson's experiment performed at 38 ℃ with different RHs (100, 95, 90, 83, and 73%). As mentioned in previous section, the values of k, ρ_{gel}, and Z were determined for free expansion case (Figure 3.2 (a)) and the same values were used for the other cases as well. Experimental results show clear RH dependency in ASR expansion progresses. Notably, the results indicate that for cases with high RHs (Figures 3.2. (a), (b), and (c)), the simulation results are in accordance with the experimental results. However, for cases with low RHs (Figure 3.2. (d) and (e)), the simulations underestimated the expansion of the mortar specimens. At this lower RH range, the value of k_{RH} in Eq. (2) was reduced. It is assumed that this gap is caused by the threshold setting in the RH dependent equation (Eq. (2)).

To evaluate this aspect, Eq. (2) was replaced with Eq. (11) to reduce the RH threshold of ASR; Figure 3.3 shows the difference between these two equations. The simulation of Olaffson's experiment [5] was conducted again with Eq. (11).

$$k_{RH} = \exp(-1500.0 \cdot (1.0 - RH)^{6.0}) \quad (11)$$

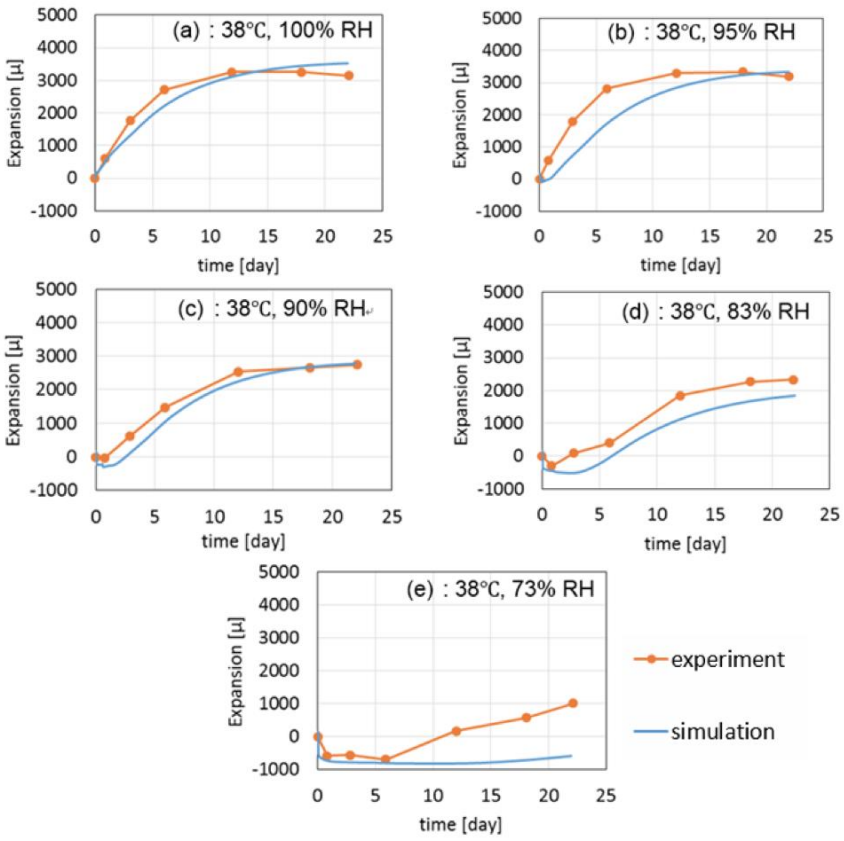

Figure 3.2: Simulation and experimental results at 38 ℃ with different RHs. Eq. (2) was used.

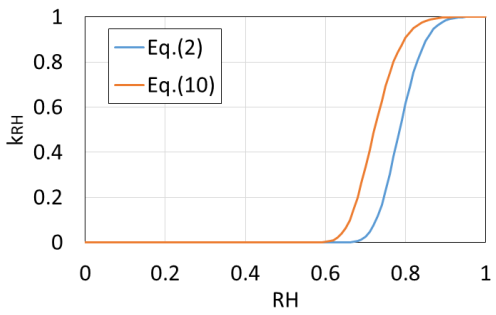

Figure 3.3: Difference between Eqs. (2) and (11)

As seen in Figure 3.4, with the new RH dependent equation, our current model can generally reflect the RH dependency of ASR at high (38 ℃). This equation can be applied to the low (23 ℃) temperature cases as well (Figure 3.4. (f), (g) and (h)). However, the RH dependency seems not the governing factor in the overestimation of the expansion of the real-scale RC bridge deck specimen shown in Figure 2.6 because the previous model underestimates the expansion at a lower RH range as shown in Figure 3.2. It is assumed that mechanisms other than RH dependency are the main cause of overestimation.

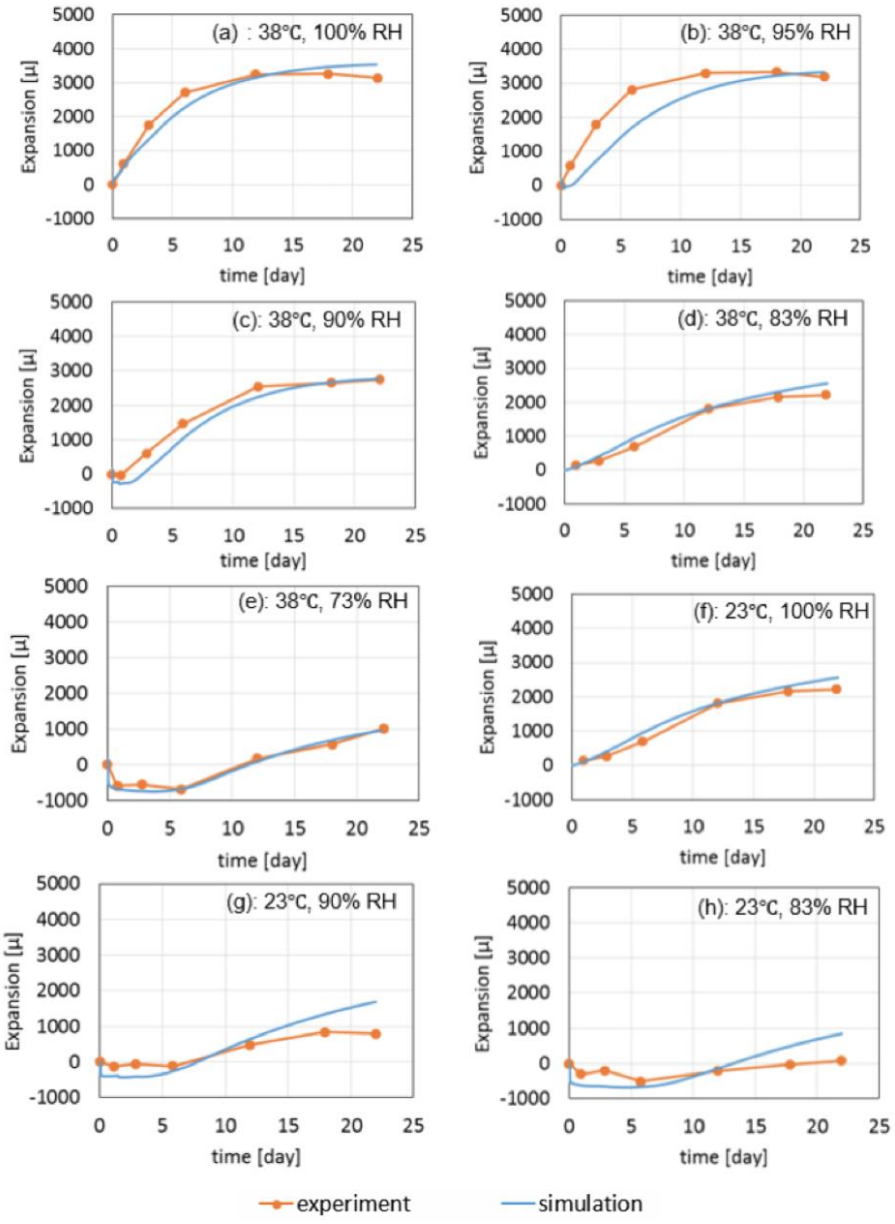

Figure 3.4: Simulation and experimental results at 38 ℃ and 23 ℃ with different RHs. Eq. (11) was used.

3.2 Simulation of ASR experiment on confinement dependency

To achieve a more comprehensive evaluation of the prediction of ASR expansion under different confinement states, the experiment performed by Gautam *et al.* [2, 7] was selected to examine the effect of confinement in the current model.

Gautam *et al.* [2, 7] measured the expansions of a group of concrete specimens under different confinement states, as shown in Table 3.2. The size of the specimens was 254 mm^3, and various three-dimensional confinements were applied using prestress bars. The mix proportion is shown in Table 3.3.

The specimens were cured for 180 days at a temperature of $\mathbf{23} \pm \mathbf{3}$ ℃ and covered with wet burlap. The conditions were changed on the 180th day to $\mathbf{50} \pm \mathbf{0.5}$ ℃ at a RH higher than $\mathbf{95}\%$, to accelerate ASR. The expansions of the specimens were measured using a digital micrometer.

Table 3.2: Average applied stress state in concrete specimens [2]

Stress state	Designation	Averaged applied stress (MPa)		
		f_x	f_y	f_z
No-stress	n (0,0,0)	0	0	0
Uniaxial	u (3.9,0,0)	3.9	0	0
	U (9.6,0,0)	9.6	0	0
Biaxial	b (3.9,3.9,0)	3.9	3.9	0
	B (9.6,3.9,0)	9.6	3.9	0
Tri-axial	t (3.9,3.9,3.9)	3.9	3.9	3.9
	T (9.6,3.9,3.9)	9.6	3.9	3.9

Table 3.3: Mix proportion used to simulate the experiment by Gautam *et al.* [2, 7]

W/C (%)	Unit weight (kg/m^3)				
	W	C	S	G	Na_2O_{eq}
44	184.8	420	719.2	1115	5.25

Simulations were performed by inputting the same mix proportions and curing and environmental conditions as those of Gautam's experiment. However, the average unit weights for coarse and fine aggregates were assumed in the simulation because no corresponding information was provided in the paper. In the experiment, confinement was applied using high-strength bolts that were tensioned until they almost yielded to keep the stress constant. More details regarding the simulation can be found in a previous paper [7]. To reproduce the confinement conditions, pre-tensioned line elements with equivalent stiffness, areas, and yield strengths as those of the bolts used in the experiments conducted by Gautam were applied to the analytical model, as illustrated in Figure 3.5, on day 52, in accordance with the experimental conditions. The impact of the confinement in one direction on the expansion in orthogonal directions were already considered in the model and verified in the previous study [3], in which the ASR-gel pressure in each direction is calculated based on the mixed solid-liquid state of ASR-gel and partial anisotropic behaviors.

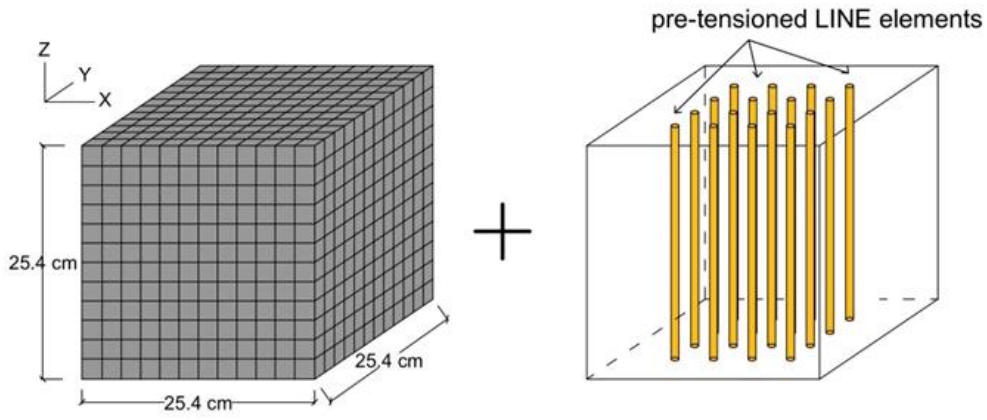

Figure 3.5: Mesh for ASR experiment on stress dependency for uniaxial stress state

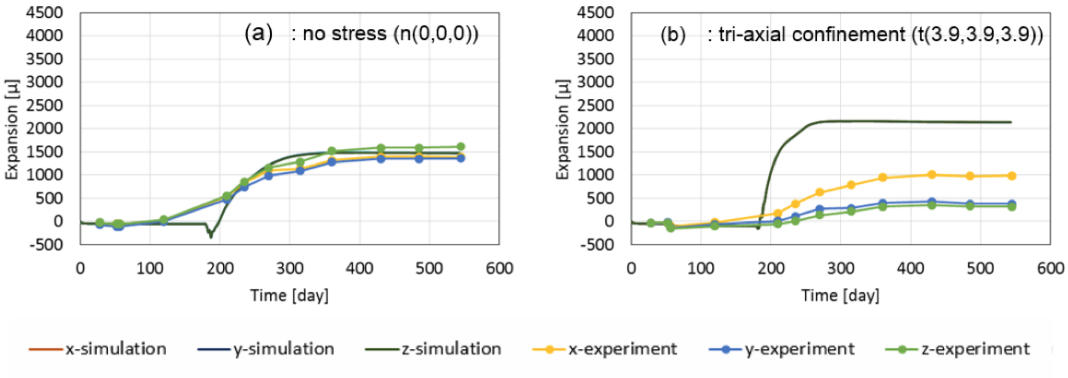

Figure 3.6: Simulation results for stress state of (a) no stress (n (0,0,0)) and (b) tri-axial confinement (t (3.9,3.9,3.9))

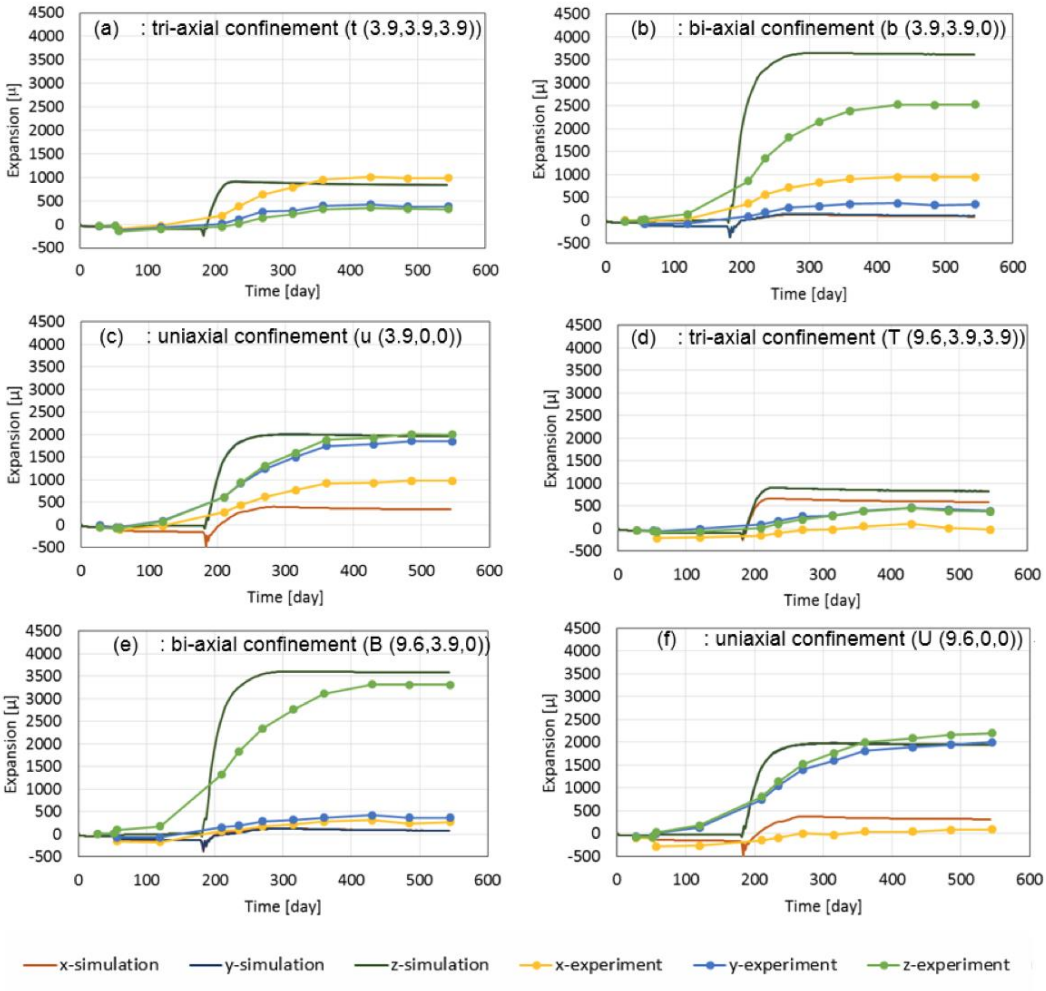

Figure 3.7: Simulation results under different stress states

Sensitivity analyses were conducted for the free expansion case to determine the following parameters: reactivity of aggregate, which is parameter k in Eq. (1), average density of ASR gel, $\boldsymbol{\rho_{gel}}$ [g/cm^3], and the coefficient Z in Eq. (6). With the values of k,$\boldsymbol{\rho_{gel}}$ and Z being 0.0007, 1.2 and 1.0, respectively, the simulated expansion progress matched the experimental progress of free expansion case as observed in Figure 3.6(a). Next, these determined parameters were used to perform the following simulations for the confined cases. Figure 3.6(b) shows the results of the triaxial cases, in which gaps appeared

between the analytical and experimental results in the confined cases with the same k, $\boldsymbol{\rho_{gel}}$, and *Z*. Then, the larger influence of confinement on gel absorption was considered by changing the coefficient *Z* from 1.0 to 0.5. As a result, the analytical results of the remaining cases with confinement were able to match the experimental results, as displayed in Figure 3.7. Eq. (6) indicates that when Z decreases, more ASR gel is absorbed into the capillary pore, and thus less expansion is observed. Considering the simulation results, it can be assumed that the compressive stress extrudes the ASR into the capillary pores and leads to less expansion. Thus, we can successfully calculate anisotropic ASR expansions of concrete under anisotropic three-dimensional stress states. Until this step, it was assumed that the incorrect prediction of the expansion of the real-scale bridge decks mentioned in Section 2 was due to insufficient consideration of the influence of confinement on ASR gel absorption.

3.3 Simulation of real-scale RC bridge deck

Based on the above assumption about the confinement effect on ASR expansion, simulations were conducted again on the real-scale RC bridge deck with a reduced *Z* parameter. In simulations of a previous research, *Z* input to the bridge deck model was 0.4, determined by sensitive analysis where the expansion of a specimen with the same mix proportion was appropriately predicted. Figure 3.8 shows the new simulation results with the Z value of 0.25, which has improved simulation results.

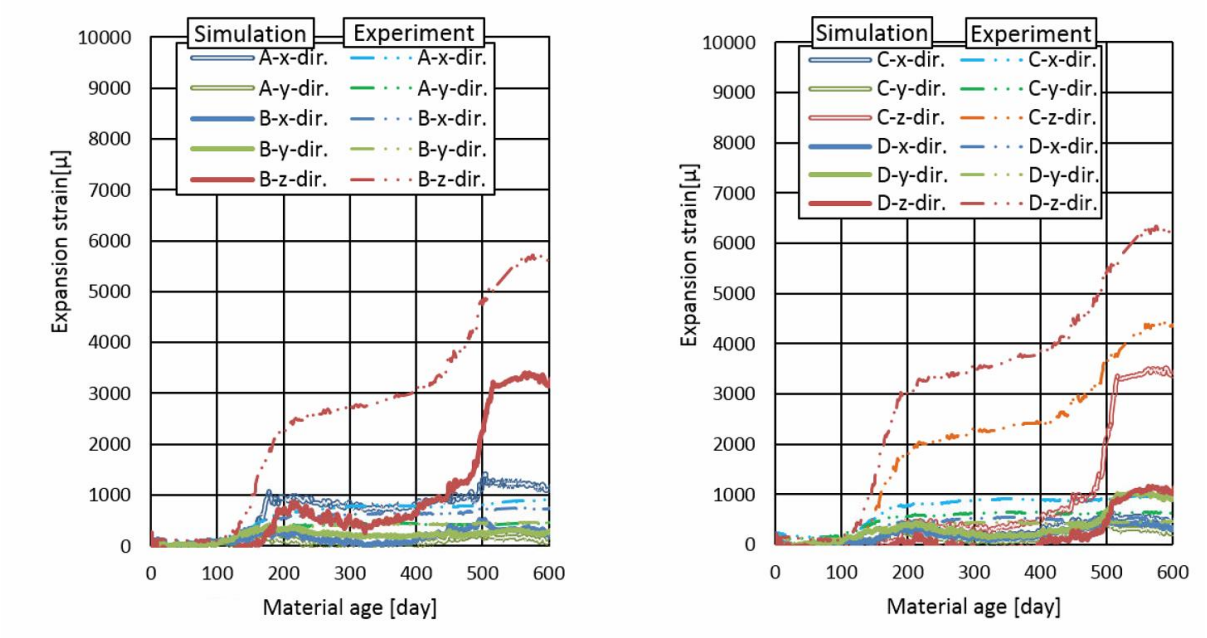

Figure 3.8: New simulation results of real scale RC bridge deck

3.4 Effect of confinement on ASR under different stress conditions

The values of *Z* utilized as inputs to the prediction model are listed in Table 3.4. From the free expansion to the confined case, the reduction of *Z* for the simulation for Gautam's specimens is higher than that in the simulation for RC bridge deck specimens.

Table 3.4: Values of *Z* used in the simulations

	Z for free expansion case	*Z* for confined case
Gautam's specimens	1	0.5
Real scale RC bridge deck	0.4	0.25

To investigate the simulation results in detail, the internal stress states inside the analytical meshes for two simulations were examined. Figures 3.9 and 3.10 show the stress contours in the simulations for Gautam's specimens and RC bridge deck specimen at their final stage of expansion, which are 211th

day and 500th day, respectively. It can be observed from Figures 3.9 and 3.10 that the compressive stresses in Gautam's case are larger than those in the RC bridge deck. The calculated internal compressive stress can be around 4 MPa at maximum in Gautam's case, while it is around 2 MPa at near steel girder in bridge deck case. Thus, it is reasonable to assume that the stronger confinement causes more ASR gel to be absorbed into the pore, and less generated ASR gel contributes to the expansion. The insufficient consideration of this aspect in the models described in Eqs. (6) and (7) leads to the inappropriate expansion prediction of RC bridge deck in the previous research [4]. To modify the model, deeper evaluation is necessary, and the corresponding mechanism should be considered in future work.

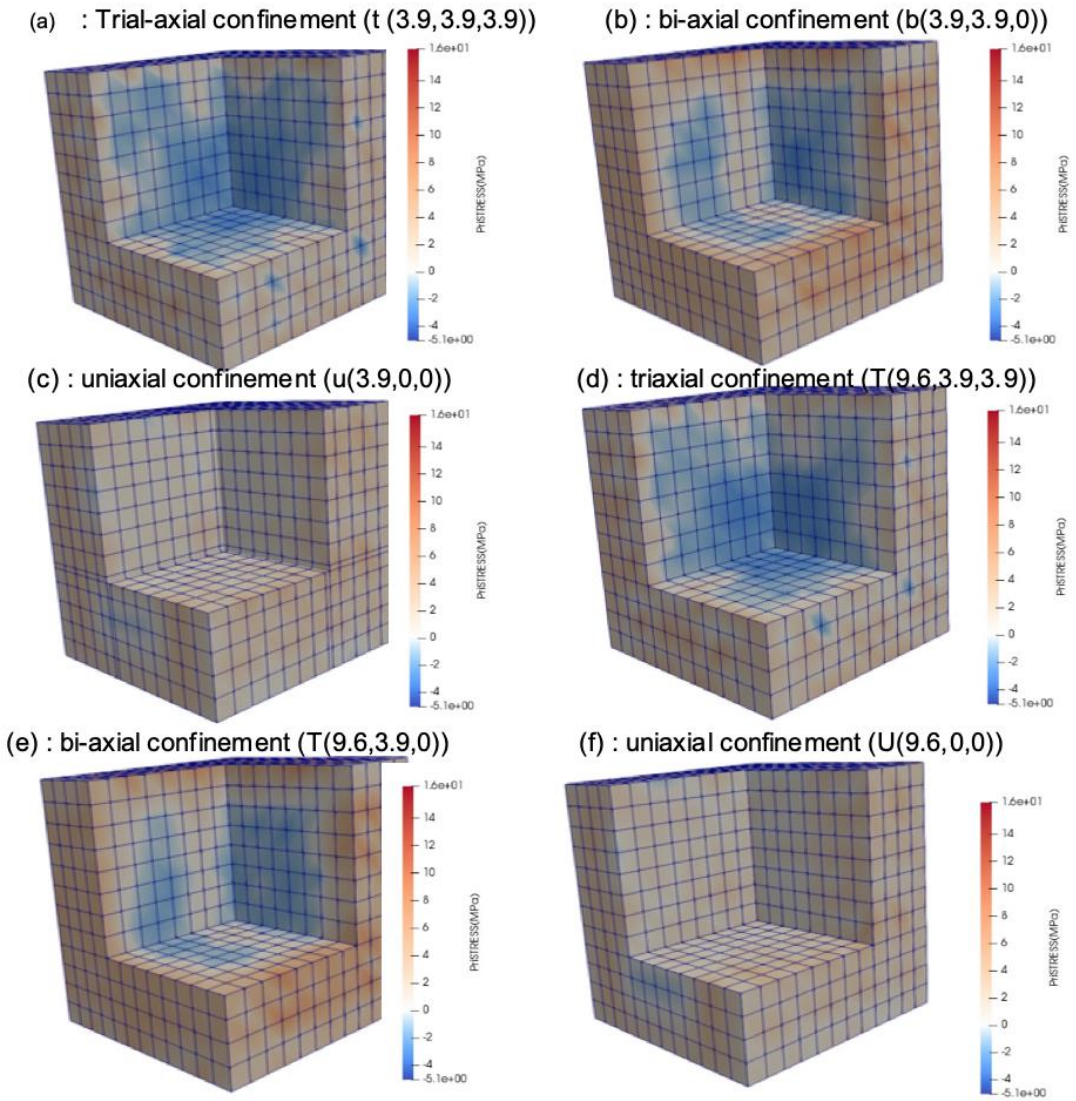

Figure 3.9: Simulated principal stress of specimens in Gautam's experiment under different stress states at surface and internal sections

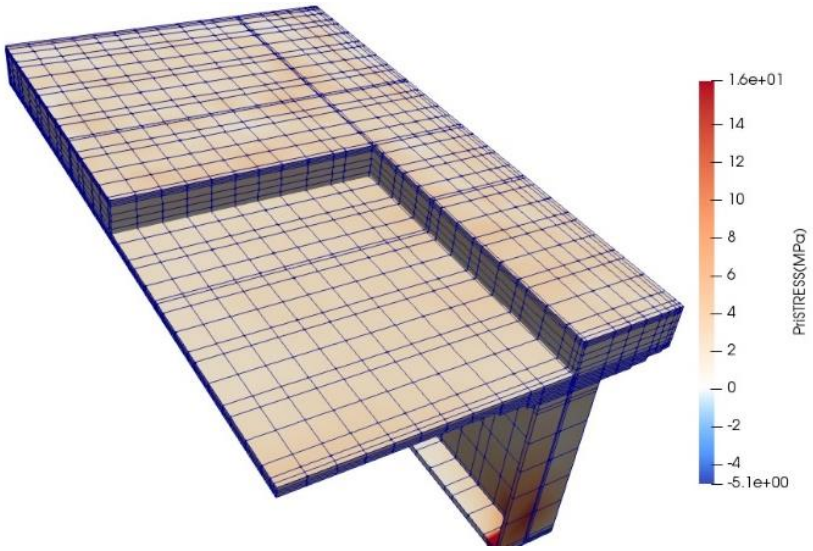

Figure 3.10: Simulated principal stress of real-scale bridge deck at surface and internal sections

4. CONCLUSION

This research aimed to improve the prediction model for alkali–silica reaction of concrete structures under real environmental and confinement conditions. Two experiments were simulated using the ASR expansion prediction model developed by the authors, focusing on temperature, relative humidity (RH), and stress dependencies. Based on the simulation results, improved model for RH dependency was introduced. And some of the problems that were observed in the previous research could be explained with the comparison of experimental and simulation results, where the expansion of a real scale bridge deck could not be quantitatively predicted by existing models. It was assumed that the prediction model did not comprehensively consider the effect of confinement, and the expansion of the real-scale RC bridge deck was overestimated. The simulation results on this bridge deck were improved by adjusting relevant parameters. To modify the prediction model, more detailed mechanism about the stress dependency of expansion needs to be studied in future research.

5. REFERENCES

[1] Deschenes Jr R A, Giannini E R, Drimalas T (2018) Effects of moisture, temperature, and freezing and thawing on alkali-silica reaction. ACI Materials Journal 115(4): 575-584.

[2] Gautam B P, Panesar D K, Sheikh S A (2017) Multiaxial expansion-stress relationship for alkali silica reaction-affected concrete. ACI Materials Journal, 114(1):171-184.

[3] Takahashi Y, Ogawa S, Tanaka Y, Maekawa K (2016) Scale-dependent ASR expansion of concrete and its prediction coupled with silica gel generation and migration. Journal of Advanced Concrete Technology 14(8): 444-463.

[4] Takahashi Y, Maeshima T, Iwaki, I, Maekawa, K (2019) An analytical study about the deformation behavior of a real scale RC bridge deck on steel girders with alkali silica reactions in real environmental conditions. Journal of Structural Engineering, 65(A): 665-673.

[5] Olafsson H (1986), The effect of relative humidity and temperature on alkali expansion of mortar bars. Proceedings of the 7th International Conference on Concrete Alkali Aggregate Reactions, Ottawa, Canada, 461-466.

[6] Maekawa K, Ishida T, Kishi T (2008) Multi-scale modeling of structural concrete, Taylor and Francis.

[7] Gautam B P (2016). Multiaxially loaded concrete undergoing alkali-silica reaction (ASR), Dissertation, University of Toronto.